Lifting the Taung child

SIR — The Taung child, *Australopithecus africanus*[1], is a key fossil to our understanding of hominid evolution. It is, however, accompanied by an exceptional fossil fauna comprised of mainly relatively small animals. This has led to much analysis and speculation about the possible agent responsible for the accumulation of this fauna[2]. Large carnivores or even the ape-man himself have been proposed as the most likely candidates. Recently, Berger and Clarke[3] suggested that the primary collecting agent of the Taung child and the associated fauna was a large bird of prey. Support for this hypothesis was obtained by comparison of the Taung fauna with that found below nests of large African eagles. The most likely candidate species is the crowned eagle *Stephanoaetus coronatus*[3], which was anecdotally reported to have attacked, and nearly killed, a 7-year-old child of approximately 20 kg. The body mass of the Taung child was probably 10–12 kg (ref. 3).

I used biomechanical information[4,5] about bird load-lifting capacity to test whether a raptor the size of a crowned eagle would be capable of carrying a prey the weight of the Taung hominid. During a short anaerobic sprint exertion, the load-lifting capacity of a crowned eagle is approximately 6.1 kg (ref. 4; assuming a 4.12-kg eagle body mass[6]), well below the body mass of the Taung child. In sustained flapping flight, the fuel load-carrying capacity of an eagle is only about 1.7 kg (ref. 5). However, because fat used as fuel is uniformly distributed around the body, drag is minimized compared with a load of prey held in the talons. Therefore, this represents an upper limit to the sustainable load-carrying capacity. The distance between the hominid savannah habitat and the deposition site was probably substantial[3], and so an eagle could have carried little more than the skull over this distance.

Biomechanics thus show that if a large bird of prey collected the Taung fauna, the Taung child itself must have been dismembered before being brought to the eagle's nest.

Anders Hedenström
Department of Zoology, University of Cambridge, Cambridge CB2 3EJ, UK

1. Dart, R. A. *Nature* **115**, 195–199 (1925).
2. Brain, C. K. *Hominid Evolution: Past, Present and Future* (ed. Tobias, P. V.) 41–46 (Liss, New York, 1985).
3. Berger, L. R. & Clarke, R. J. *J. hum. Evol.* **29**, 275–299 (1995).
4. Marden, J. H. *J. exp. Biol.* **149**, 511–514 (1990).
5. Hedenström, A. & Alerstam, T. *J. exp. Biol.* **164**, 19–38 (1992).
6. Brown, L. H., Urban, E. K. & Newman, K. *The Birds of Africa* Vol. 1 (Academic, London, 1982).

Energetic motion detection

SIR — Motion detection has been widely investigated using random-dot kinematograms (RDKs). Under appropriate conditions, motion may be seen between a random-dot image and its displaced counterpart[1]. Here we attempt to discriminate between the two classes of model that can account for this.

Proponents of energy-based models argue that low-level motion sensors detect motion energy at a range of spatial scales[2]. The directional outputs of the detectors are later combined to indicate the overall direction of movement of an object. Alternatively, edge-based models suggest that the edges in an image are located and then motion is detected at a single scale by forming correspondences between displaced edges[3]. Both models can account for the observation that the maximum displacement for motion detection (d_{max}) increases when a RDK is low-pass filtered. For energy-based models, this is because low-spatial-frequency detectors have larger receptive fields and tolerate larger spatial displacements. For edge-based models the increase is because low-pass filtering increases the separation between edges.

d_{max} is surprisingly small for white noise, given the presence of low spatial frequencies[1], while the absence of an effect on d_{max} of initial low-pass filtering is unexpected[4]. Proponents of energy-based models must resort to special pleading to explain these effects (that is, that high spatial frequencies mask low[4]). In edge-based models, direction discrimination is based on the edges in the pattern after initial blurring by the visual system. The low-pass filtering of the stimulus must exceed that of the visual system before there is any noticeable effect. A cornerstone of the argument supporting edge-based models is the recent finding that observers could not see motion between a binary noise image and some of its low-pass-filtered counterparts[5]. In these images, there is little correspondence between the location of the edges in the two frames, so edge-based models predict that motion would not be detected. There is motion energy at common (low) spatial frequencies, however, so energy-based models predict that motion would be seen.

White-noise patterns in RDKs generally contain equal energy at all spatial frequencies. It has been suggested that the spatial characteristics of cortical cells are matched to the spectra of natural images, thus providing an efficient representation of the natural environment[6,7]. Both simple and complex cortical cells have frequency bandwidths that are approximately constant in octaves[8,9]. Thus, white-noise patterns produce activity skewed towards high spatial frequencies because the frequency bandwidth of cortical cells increases with peak frequency; cells tuned to high spatial frequencies respond the most. To provide a more appropriate test, noise patterns were filtered to the $1/f$ magnitude spectrum characteristic of natural images, where magnitude scales inversely with spatial frequency. The response of visual cortex cells to $1/f$ patterns is therefore equal across spatial scales and the neural representation is broad and flat.

We measured d_{max} using $1/f$ noise patterns which were subsequently low-pass filtered or high-pass filtered (Fig. 1, top row). The observer reported the direction of displacement in each trial. Direction

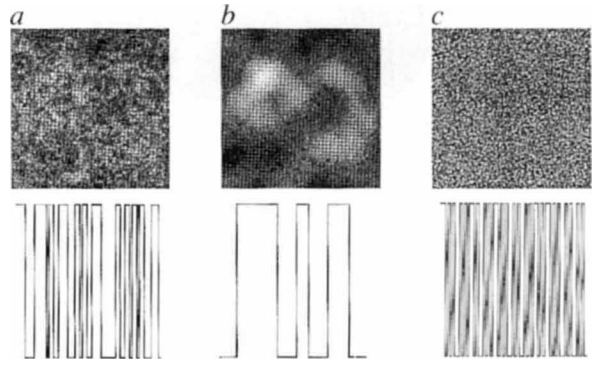

FIG. 1 The top row illustrates stimuli used. *a*, An 8-bit (gaussian) white-noise field, filtered to have a $1/f$ relationship between spatial frequency and amplitude; *b*, low-pass-filtered version of *a*; *c*, high-pass-filtered version of *a*. Contrast has been normalized for illustrative purposes, but in the experiment contrast was not normalized. The second row shows the edges in a one-dimensional section through each noise sample after low-pass filtering to simulate visual blurring. The edges were located at the zero crossings in the second spatial derivative of the blurred luminance profiles[12]. There is little correlation between the edges in each pattern, and any edge-matching algorithm would be unable to identify correct matches for motion detection between filtered and unfiltered $1/f$ patterns. It may be possible to match the peaks between the $1/f$ and the low-pass image, but it would not be possible to match them between the $1/f$ and the high-pass image. Four main conditions were examined: both images were filtered in the same cut-off (low- or high-pass); one image was $1/f$ noise and the other was filtered (low- or high-pass). The order in which the images were presented was examined separately (full experimental details are available on request). Direction discrimination was possible between broad-band $1/f$ noise and filtered $1/f$ noise, despite the absence of correlation between the edges in these images.

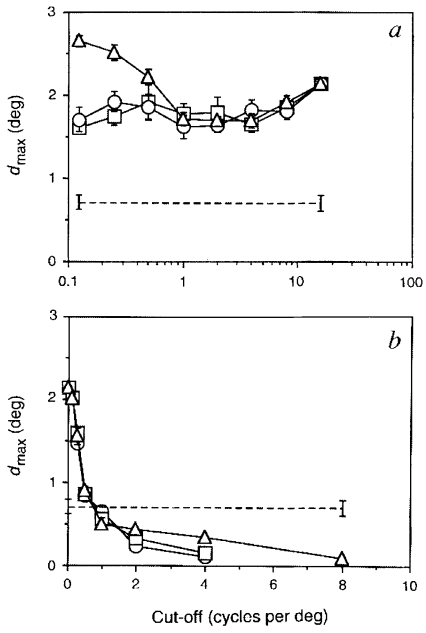

FIG. 2 d_{max} as a function of the cut-off frequency of filtered $1/f$ noise patterns. d_{max} corresponds to the displacement at which there were 20% errors in direction discrimination. The data are shown for a naive observer (similar data are available on request for a second observer). *a*, Low-pass data; *b*, high-pass data. The cut-off of the filter is shown on the *x*-axis in cycles per degree. For the low-pass condition, 16 c deg^{-1} represents the unfiltered $1/f$ noise pattern (the Nyquist limit of the image). For the high-pass condition, 0 c deg^{-1} represents the unfiltered $1/f$ noise pattern. Graphs show estimates of d_{max} when: both images were filtered (Δ); when the first image was broad-band ($1/f$) and the second was filtered (□); and when the first image was filtered and the second was $1/f$ (○). The broken line shows the estimate of d_{max} for the unfiltered 8-bit noise. Error bars show ± 1 s.e.; d_{max} was relatively unaffected by low-pass filtering except when the cut-off was very low, where there was a slight increase in the mixed image sequence. When either image was high-pass filtered, d_{max} scaled with the lowest spatial frequencies in the high-pass image. Observers could not see motion between unfiltered $1/f$ noise and high-pass patterns with the highest cut-off, which may be related to the low contrast of the high-pass-filtered image.

discrimination was measured for displacements between two images which were either both filtered or only one of which was filtered (the other was $1/f$). When one of the images was filtered and the other was broad-band, direction discrimination was possible under almost all conditions (Fig. 2). In these images, there was little or no correlation between the edges in each image (Fig. 1, bottom row), but there was motion energy at common spatial scales. Furthermore, motion may be seen between unfiltered $1/f$ and band-pass-filtered $1/f$ patterns of various central frequencies, suggesting that the human motion system has equal access to information across spatial scales for natural images[10].

Although direction discrimination may, in principle, be performed by a high-level feature-tracking mechanism[11], this cannot explain motion detection between unfiltered and filtered images. These results show that low-level motion detectors are energy-based and reconcile the different explanations of the lack of effect on d_{max} of initial low-pass filtering. Such results are expected when the response bias to high spatial frequencies in white noise patterns is considered. The neural representation of white noise is effectively high-pass-filtered. It is therefore unsurprising that high spatial frequencies are dominant and that motion may not be seen between white noise patterns and their low-pass-filtered counterparts. Although there is undoubtedly initial low-pass filtering due to the limited resolution of the visual system, the separation between edges in the neural representation of an image cannot account for the ability to integrate motion between images whose edges are uncorrelated.

Peter J. Bex*
N. Brady
R. E. Fredericksen
R. F. Hess
McGill Vision Research Unit,
Department of Ophthalmology,
McGill University, 687 Pine Avenue West,
Montreal H3A 1A1, Canada

MORGAN REPLIES — Mather and I[5] showed that motion detection is possible between pairs of random noise patterns, one of which has been low-pass-filtered (blurred), even though the appearance of the blurred and unblurred patterns is distinctly different. This was explained by a motion-detection model in which the patterns are matched following a visual filtering stage in which high-spatial-frequency components are substantially attenuated[3]. After filtering, the initially blurred and initially unblurred patterns have a spatial structure that matches sufficiently closely for motion to be detected. Only when the difference in blur is extreme does the matching process break down, and detection by human observers fail[5].

Bex *et al.* have now shown that correct matching can also be achieved between filtered and unfiltered versions of a $1/f$-scaled gaussian noise pattern. Scaling by $1/f$ selectively attenuates high spatial frequencies, and so would be expected to reduce the effects of subsequent low-pass filtering, as Bex *et al.* find. Their result

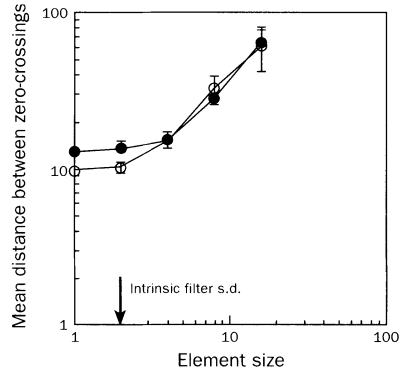

FIG. 3 The zero-crossing structure of random binary noise viewed through a filter that attenuates high spatial frequencies is little affected by $1/f$ filtering. The noise consisted of elements that were white or black with equal probability and which had the size shown on the abscissa. (Similar results are obtained with gaussian noise as used by Bex *et al.*) The noise pattern was convolved with a laplacian-of-gaussian filter with a standard deviation of 2 units, and the mean distance between zero-crossings was measured (ordinate). ○, Unscaled; ●, $1/f$ -scaled. There were 10 independent simulations for each data point and the vertical bars represent standard deviations. For further details of the model see ref. 3.

would be expected if the spatial structure of the filtered and unfiltered patterns were sufficiently correlated following further filtering by an intrinsic visual filter. A simple statistical description of the edge structure of a noise pattern is provided by the mean distance between zero-crossings in the second spatial derivative[13]. This statistic is substantially unaffected by $1/f$ filtering (Fig. 3), except that, at small element sizes, the interval is about twice as great for $1/f$-filtered patterns, in agreement with Bex *et al.*'s finding that the $1/f$ patterns have two to three times larger d_{max} values than pure noise. We predict that this difference would disappear with larger element sizes. The value of d_{max} for pairs of white noise should not be increased by $1/f$ filtering of one of the pair. If either of these two predictions is wrong, our model could be rejected.

The opposition that Bex *et al.* propose between 'motion energy' and 'edge matching' models of motion detection does not necessarily reflect different mechanisms. The zero-crossing pattern is a convenient description of its statistical structure, which is basic for understanding its effects, whether on a motion-energy detector or otherwise. In describing the

1. Braddick, O. J. *Vision Res.* **14,** 519–527 (1974).
2. Adelson, E. H. & Bergen, J. R. *J. opt. Soc. Am. A* **2,** 284–299 (1985).
3. Morgan, M. J. *Nature* **355,** 344–346 (1992).
4. Cleary, R. & Braddick, O. J. *Vision Res.* **30,** 317–327 (1990).
5. Morgan, M. J. & Mather, G. *Vision Res.* **34,** 197–208 (1994).
6. Field, D. J. *J. opt. Soc. Am.* **A4,** 2379–2394 (1987).
7. Brady, N. & Field, D. J. *Vision Res.* **35,** 739–756 (1995).
8. De Valois, R. L., Albrecht, D. C. & Thorrel, L. G. *Vision Res.* **22,** 545–559 (1982).
9. Tolhurst, D. J. & Thompson, I. D. *Proc. R. Soc. Lond.* B**213,** 183–199 (1981).
10. Brady, N., Bex, P. & Fredericksen, R. E. *Vision Res.* (submitted).
11. Cavanagh, P. *Science* **257,** 1563-1565 (1992).
12. Marr, D. & Hildreth, E. *Proc. R. Soc. Lond. B* **7,** 187–217 (1980).
13. Marr, D., Ullman, S. & Poggio, T. *J. opt. Soc. Am.* **69,** 914–916 (1979).
14. Morrone, M. C. & Burr, D. C. *Proc. R. Soc.* B**235,** 221–245 (1990).

* Present address: Center for Visual Science, University of Rochester, 274 Meliora Hall, Rochester, New York 14627, USA.